

## Footstep planning for slippery and slanted terrain using human-inspired models

Martim Brandão, *Member, IEEE*,  
 Kenji Hashimoto, *Member, IEEE*,  
 José Santos-Victor, *Member, IEEE*,  
 and Atsuo Takanishi, *Member, IEEE*

**Abstract**—Energy efficiency and robustness of locomotion to different terrain conditions are important problems for humanoid robots deployed in the real world. In this paper we propose a footstep planning algorithm for humanoids applicable to flat, slanted and slippery terrain which uses simple principles and representations gathered from human gait literature. The planner optimizes a center-of-mass (COM) mechanical work model subject to motion feasibility and ground friction constraints using a hybrid A\* search and optimization approach. Footstep placements and orientations are discrete states searched with an A\* algorithm, while other relevant parameters are computed through continuous optimization on state transitions. These parameters are also inspired by human gait literature and include footstep timing (double support and swing time) and parameterized COM motion using knee flexion angle keypoints. The planner relies on work, required coefficient of friction (RCOF) and feasibility models that we estimate in physics simulation.

We show through simulation experiments that the proposed planner leads to both low electrical energy consumption and human-like motion on a variety of scenarios. Using the planner, the robot automatically opts between avoiding or (slowly) traversing slippery patches depending on their size and friction; and it chooses energy-optimal stairs and climbing angles in slopes. The obtained motion is also consistent with observations found in human gait literature, such as human-like changes in RCOF, step length and double support time on slippery terrain, and human-like curved walking on steep slopes. Finally, we compare COM work minimization with other choices of objective function.

**Index Terms**—Biologically-Inspired Robots, Humanoid Robots, Motion planning, Footstep planning, Path planning, Human gait

### I. INTRODUCTION

**H**UMANOID robot locomotion planning is an important problem with applications in disaster response and service. Footstep planning algorithms are a computationally attractive solution to the locomotion problem since they reduce the search space from whole-body motion to footstep positions and orientations. Current footstep planners excel at obstacle avoidance, but do not consider important factors such as ground friction and energy consumption. These are especially important in outdoor environments where the robot will depend on batteries and surface conditions might be challenging: slippery, inclined, etc. While it is still not clear how footstep planners should be formulated in order to consider many of such factors, our claim in this paper is that using principles and representations in human gait literature can lead to natural improvements of footstep planning. Namely, in this paper we integrate human-inspired COM work and RCOF models as functions of footstep displacement, timing and parameterized COM motion, into a new hybrid search-optimization planner: obtaining friction-aware low-electrical-power footstep plans.

M. Brandão is with the Graduate School of Advanced Science and Engineering, Waseda University.

K. Hashimoto is with the Waseda Institute for Advanced Study, and is a researcher at the Humanoid Robotics Institute (HRI), Waseda University.

J. Santos-Victor is with the Institute for Systems and Robotics, Instituto Superior Técnico, Universidade de Lisboa.

A. Takanishi is with the Department of Modern Mechanical Engineering, Waseda University; and the director of the Humanoid Robotics Institute (HRI), Waseda University.

Manuscript received xxx, 2015; revised xxx, 2016.

The contributions of this paper are the following: 1) We give an overview of anticipatory human gait literature, and identify principles and representations useful to humanoid locomotion in a variety of scenarios; 2) We propose a footstep planning algorithm based on 1 which plans both footstep positions, orientations, timing and parameterized COM motion; 3) We show that the proposed method applied to the WABIAN-2 robot leads to walking motion observations consistent to those seen in human gait literature; and 4) We show that paths obtained with the proposed planner also lead to low electrical energy consumption.

This paper is related to two previous publications [1], [2]. Compared to these we: 1) Further extend the models and planner to account for locomotion on slopes; 2) Give an overview of anticipatory human gait literature relevant to footstep planning, explaining the motivations behind our choice of optimization objectives, constraints and variables; 3) Claim human-likeness of the motion obtained with our planner by comparing it with observations in human gait.

### II. RELATED WORK

#### A. Humanoid footstep planning

In humanoid walking, as in human gait literature, it is common to distinguish two levels of locomotion control: planning and feedback control. In this paper we focus on the (footstep) planning problem for humanoids. This problem is closely related to the study of anticipatory human gait adaptations. For example, representations of walking used in human gait literature to describe anticipatory gait control are closely related to those used in high-level motion planning algorithms in robotics, such as footstep planning, contact planning and other task-space planning approaches. Both typically deal with observations in terms of a high-level representation of walking such as modality, foot position, orientation, timing, limb stiffness or center-of-mass (COM) height.

For humanoids, the footstep and contact planning problems have been tackled with search [3], [4], [5], [6], [7], sampling [8] and optimization [9], [10] algorithms. Search-based planners such as A\* [3], [4], [5] and its variants [6], [7] have been used successfully to plan obstacle free paths in both static and dynamic [5] scenarios. Recently, purely optimization-based planners have also been proposed [10], which eliminate the sub-optimal discretization problem inherent to search-based planners. Sampling-based [8] planners allowing for multiple contacts (e.g. hands, knees) are useful for very complex environments, although at a high computational cost, which can be slightly ameliorated with a good selection and adaptation of motion primitives [11]. While the aforementioned planners focus on finding collision-free paths, the methods in this paper go one step further: considering energy, collision and friction.

One important step in footstep planners is to estimate whether a given stance or step is feasible or not. Some authors opt to approximate feasibility by rough reachability of the feet [7], full inverse kinematics feasibility [8], or smart collision checking [12]. In this paper we use both rough reachability intervals to discard obvious unfeasible poses, as in [7], but also learn a model of feasibility from physics simulation: where feasibility is both static and dynamic.

Research closely related to this paper includes [3], in which terrain and energy-related cost functions are used in A\* search to compute optimal cost plans. They sum a set of empirical human biomechanics-inspired models of energy cost that are polynomial functions of step length, width and rotation. Also [4] uses a similar approach, with quadratic cost functions on sequences of footstep positions. On the other hand, in this paper we consider also timing variables and surface

friction. We do not assume polynomial relationships and instead use an off-the-shelf machine learning algorithm to learn the relationship between variables from data. And finally we make claims concerning energy consumption and human-like motion.

In this paper we prevent slippage of the robot by planning, which complements other feedback control approaches to friction-constrained biped walking [13], [14], [15]. While feedback control can help reduce tangential-to-normal force ratios locally, it may not be sufficient in very low friction surfaces. For example a robot with rubber soles would be subjected to less than 0.15 kinetic friction when walking on ice. Slipping can be reduced in such low friction floors without changing gait, but not eliminated [13]. Feedback control approaches usually consist of friction cone constraints in inverse dynamics [16] or operational space control framework [15]. Design parameters in the preview controller [17] can also be slightly tuned to reduce the RCOF for a fixed gait, and feedback ZMP controllers manually adapted to account for friction [13]. Efforts have also been put into reactive reflex controllers that, without changing gait parameters, try to reduce slipping after it is detected (e.g. by waist or foot acceleration reflexes [14]). In this paper we take the complementary high-level approach, by optimizing energy and eliminating slippage as much as possible by changes in gait. Such approach solves the known problem of reactive controllers to not be able to avoid slipping on fast gait [14], and at the same time leverages on human gait literature findings supporting energy and stability optimization at the footstep level, which is not just reactively but also anticipatorily controlled.

#### B. Anticipatory gait control in humans: human gait is planned

The claim that humans also plan gait, and footsteps in particular, is supported by several evidence in both children and adults. For example, children walkers (average 14 months) switch walking modality from bipedal to quadrupedal on a waterbed after visual inspection of its waviness or haptic exploration [18]. Children also use haptic exploration on slopes to decide whether to walk, crawl, slide down in sitting or backing positions or not traverse them at all [19].

Across numerous studies of adult human walking there is also the observation of a "cautious gait" style used in uncertain environments [20], [21], [22] or after sensory loss [23], [24]. For example [20], [21], [22] observed a specific cautious gait mode when there is awareness of a slippery surface, which is then adapted to the specific slipperiness condition found. Typically on slippery surfaces, walking speed is decreased, the COM is centered over the supporting limb and limb stiffness is increased [20], [21], [22]. Even when there is no knowledge of the degree of slipperiness, stride length [20], [21], [25], foot contact angle [26], [22], [27], [25] and vertical heel contact velocity [26] decrease, while knee flexion increases [22], [27]. According to [22], these surface-approach changes are learned over prior slip experience and are applied to different conditions when surface properties are unknown. Further knowledge of the coefficient of friction changes muscle activation and how the foot interacts with the floor. On slippery terrain, both these gait and muscle activation patterns become characteristically different since the first step on the surface, which indicates an anticipation strategy and not reactive adaptation of normal gait. A cautious gait is also used in other uncertain circumstances such as when vision is blurred by light scattering lenses [23]. Another interesting observation is that human walking trajectories on steep slopes such as mountains or hills are not straight least-distance paths but more energy-efficient curved paths uphill [28], [29]. Interestingly, [30] showed that visual perception of slant changes from viewpoint (downhill looks steeper and is also more difficult), which suggests that climbing gradients could be a result of perception of slant.

All these examples show how humans adapt high-level gait parameters such as modality, footstep position and timing or COM trajectories by some sort of motion planning based on visual or haptic perception of the environment.

Part of these observations have been obtained in robotics and animation literature by optimization algorithms, for example lower step lengths [1], [31] and lower COM [31] on slippery terrain. [31] achieved this by a low-level joint controller, while [1] used a footstep planning algorithm. The latter, planner-based approach is more easily adaptable to complex terrain with obstacles and slopes. In this paper we extend its methods further, obtaining several human-like walking behavior observations both in slippery terrain and slopes.

#### C. Human gait as optimization in high-level representation: variables and objectives

The optimal gait of humans, according to [28], is related to fitness of the species and is a function of several factors such as speed, acceleration, endurance, energy and stability. Human gait studies have shown that these can be modeled by simple principles and using equally simple high-level representations of gait. For example, step length and cadence have been shown to have a linear relationship [32]. Also, simple empirical equations of step length and step rate proposed by [33] lead to contours of energy consumption per meter which match subject data from different studies. In particular, the metabolic "cost of transport" (energy per unit distance) is a frequent optimization objective studied in human gait literature. Humans have been shown to choose an average step length and frequency that minimizes average energy cost per distance [33], [34], [35], [36]. Minimization of vertical cost of transport, mainly by regulation of COM height, also explains locomotion patterns on steep slopes as shown by [29]. Studies usually model energy as oxygen consumption [33], joint or muscular work [37] and body or COM work [38]. Energy recovery [39] of the COM is also another considered objective related to COM work.

The previously stated measurements have been shown to vary systematically with high-level gait parameterizations such as step length [40], [19], [21], [20], [25], step width [25], speed [40], [20], [27], COM height [20], knee flexion at heel strike [22], foot angle and velocity at heel strike [21], [26], [41], [25], double support and swing times [32], [41], [27], and limb stiffness [20]. The same variables have also been shown to be used, whether directly or indirectly, to regulate the Required Coefficient of Friction (RCOF): the ratio of shear to normal ground reaction force (i.e. tangential to normal force) [22], [21], [20]. The RCOF constraint should be kept below the ground's coefficient of friction to avoid slips and consequent falls, but it is planned and not just controlled reactively [20].

Travel time, acceleration and orientation error are also other functions which can be optimized to predict COM trajectories in flat goal-directed paths indoors [42].

### III. OUR HUMANOID FOOTSTEP PLANNING MODEL

From the anticipatory gait control studies mentioned in the previous section we selected simple optimization objectives and variables such that: 1) They are easily applicable to current humanoid locomotion planning algorithms, namely footstep planning; 2) They predict walking behavior observations in different human gait literature for a variety of scenarios. In particular we focus on observations on slippery environments, flat and slanted terrain.

Based on these criteria we selected the following optimization variables: **Step length, width and height**. As discussed in Section II-C, both energy and RCOF have been shown to vary systematically with these variables. Also, their application to robot footstep planning

is straight-forward since these are simple distances between feet. **Double support time and leg swing time.** As discussed, these vary systematically in adaptations to slippery terrain. Inclusion in (extended) footstep planning adds flexibility to the planner to lower gait accelerations and may thus allow the robot to navigate more slippery terrain, as initially proposed in [1]. **Knee flexion angles.** These also vary systematically in adaptations to slippery terrain [22]. Furthermore, they are related to COM height which explains adaptations in steep slopes and slippery terrain. For robot locomotion, planning COM trajectories is also crucial for stability and feasibility considerations. In this paper we parameterize the COM height trajectory through inflexion points of a knee angle trajectory spline.

Regarding optimization objectives and constraints, we define them and learn them in simulation as functions of the previously stated variables. The models we borrow from human gait literature are: **COM work as optimization objective.** As discussed in Section II-C, energy optimization and in particular COM work explains walking patterns in both flat and sloped terrain [35], [29]. The advantage of this model for robotics when compared to, for example, electrical energy or torque minimization is basically its simplicity. Since only COM velocity and force profiles are required to estimate COM work, it applies to both complex robot models and simple single-mass robot models. There is also the motivation of passive dynamic walkers [43] which optimize COM work by construction. **RCOF as a constraint.** As discussed, RCOF has been shown to vary on slippery terrain. While it is not clear whether RCOF should be used as a hard or soft constraint in order to explain human data, in this paper we opt for a hard constraint. We assume Coulomb friction and set  $\text{RCOF} < \mu$  as a constraint in the problem, which is advantageous from a conservative perspective: in order to theoretically avoid slipping and thus not having to rely heavily on reactive slippage control.

As we will show in the Section VI, our footstep planning model leads to the following human-gait-predicted behavior:

- Energy contours are hyperbolic in step length-rate [33], [35],
  - RCOF is reduced on slippery terrain [21],
  - Step length is reduced on slippery terrain [20], [21], [25],
  - Double support time is increased on slippery terrain [27],
  - There is an optimal climbing angle for steep slopes [28], [29].
- In other words long steep trajectories will be curved.

#### A. Problem statement

We consider the problem of finding a sequence of  $N$  footsteps  $f_j = (x_j, y_j, z_j, \theta_j) \in \mathbb{R}^4$ ,  $j = 1, \dots, N$ , such that energy is minimized and with feasibility and no-slippage as constraints. The plan starts at a fixed initial stance  $s_1 = (f_1, f_2)$  and finishes at a fixed goal stance  $s_{N-1} = (f_{N-1}, f_N)$ .  $N$  is unknown;  $(x_j, y_j, z_j)$  and  $\theta_j$  are position and yaw orientation of a foot in a global coordinate frame; for convenience  $f_j$  is a left foot if  $j$  is odd, right if  $j$  is even. The energetic cost  $E_{\text{COM}}$  of transitioning from a stance  $s_{j-1}$  to  $s_j$  depends on both the stances and some extra parameters  $p_j \in \mathbb{R}^p$ .  $p$  represents state transition parameters that might provide different ways for  $s_j$  to be reached from  $s_{j-1}$ , such as step timing and COM motion. In this paper we use  $p_j = (\Delta t_{ds}, \Delta t_{sw}, \phi_0, \phi_{st}, \phi_{sw}) \in \mathbb{R}^5$  which are double-support time (i.e. time spent on  $s_{j-1}$ ), swing time (i.e. time spent with the swing leg in the air), and minimum knee flexion, maximum stance knee flexion and maximum swing knee flexion angles. Throughout the paper we will also refer to a state (i.e. stance) transition by a "step".

The general problem we are trying to solve in this paper is

$$\begin{aligned} & \underset{N, f_3, \dots, f_{N-2}, p_2, \dots, p_{N-1}}{\text{minimize}} && \sum_{j=2 \dots N-1} E_{\text{COM}}(f_{j-1}, f_j, f_{j+1}, p_j) \\ & \text{subject to} && \\ & && \text{RCOF}(f_{j-1}, f_j, f_{j+1}, p_j) < \min(\mu_{j-1}, \mu_j, \mu_{j+1}) \\ & && \Psi(f_{j-1}, f_j, f_{j+1}, p_j) < 0 \\ & && a < p_j < b \end{aligned} \quad (1)$$

where the function  $\Psi$  implements feasibility constraints on the stances and steps due to kinematic, dynamic or controller limitations. We assume coefficient of friction  $\mu_j$  is known for each  $f_j$ , and a Coulomb friction model so that RCOF is a tangential-to-normal force ratio. Bound constraints on the step parameters are implemented with vectors  $a$  and  $b$ .

### IV. OBTAINING ENERGY, RCOF AND FEASIBILITY MODELS

#### A. Definitions

We compute total COM mechanical work as:

$$E_{\text{COM}} = \int_{t_0}^{t_1} |\mathbf{v} \cdot \mathbf{F}| dt, \quad (2)$$

where  $\mathbf{v}$  and  $\mathbf{F}$  are the velocity and total force vectors at the COM, respectively, and  $t_0, t_1$  the beginning and ending time of a step (i.e.  $t_1 - t_0 = \Delta t_{ds} + \Delta t_{sw}$ ).

RCOF [21] is defined as the maximum ratio of tangential-to-normal force applied at the feet during a given step:

$$\text{RCOF} = \max_{t \in [t_0; t_1]} \left| \frac{F_T(t)}{F_N(t)} \right| \quad (3)$$

where  $F_T$  is the tangential force and  $F_N$  normal force at the feet. In this paper we assume a Coulomb friction model. Therefore, note that if RCOF is lower than the actual coefficient of friction between feet and floor, slippage is theoretically prevented during that step.

Finally we define the feasibility model as  $\Psi \in \{-1, 1\}$  and use value 1 for unfeasible points and  $-1$  for feasible. To discard obvious unfeasible stances we first use a footstep parameterization as in [7] to obtain a heuristic approximation of footstep reachability: in a stance  $s_j$ , reachability is approximated by a set of intervals for the variables  $(\Delta x_{j+1}, \Delta y_{j+1}, \Delta z_{j+1}, \Delta \theta_{j+1})$ , which are distances from the first footstep to the second, i.e.,  $\Delta x_{j+1} = x_{j+1} - x_j$ , etc. Stances outside these intervals are considered unfeasible with  $\Psi = 1$ . Steps are also considered unfeasible if COM motion respecting the reference ZMP trajectory cannot be found using our Walking Pattern Generator [44], joint limits are reached or the robot falls during physics simulation.

#### B. Implementation

During a training stage we run physics simulations exploring the space of steps  $(f_{j-1}, f_j, f_{j+1}, p_j)$  and collecting measurements of  $E_{\text{COM}}$ , RCOF and  $\Psi$ . Each simulation consists of a symmetric and periodic gait of steps with constant step length, width, height and  $p$ . The patterns also start and finish with zero COM velocity and are stabilized with the Pattern Generator described in [44]. We train an Infinite Mixture of Linear Experts (IMLE) [45] for each model as a function  $\hat{f} : \mathbb{R}^{3+p} \rightarrow \mathbb{R}$  where inputs are the variables mentioned previously (i.e. step length, width, height and  $p$ ) and outputs are the measurements  $E_{\text{COM}}$ , RCOF and  $\Psi$ . Since the simulations consist of symmetric periodic gait, step lengths (usually defined as the distance between two consecutive feet at heel strike [22]) are the same as stance lengths, and likewise for width and height.

We chose to use IMLE for function approximation due to its high query speed and low number of experts, while still allowing for online

learning if necessary. Error performance is comparable to that of Gaussian Processes [45]. Models were trained by uniform sampling of the input space and using the necessary number of experts to obtain a standardized mean squared error (SMSE) lower than 0.1.

In the case of the feasibility function, we still fit a continuous mixture model even though training points are discrete  $\Psi \in \{-1, 1\}$ , leading to interpolation regions between  $-1$  and  $1$ . While planning, we enforce a slightly conservative feasibility constraint of  $\Psi < 0$  to avoid uncertain regions far from feasibility ( $\Psi = -1$ ).

## V. SOLVING THE PLANNING PROBLEM

### A. Discretized search of footsteps, continuous optimization of step parameters

In this paper we solve (1) by a hybrid discrete search and continuous optimization-based planner. We first constrain the footstep (position) space to a point cloud of traversable points  $(x, y, z) \in \mathbb{R}^3$  and a discrete set of orientations in the global coordinate frame:  $\theta \in \{0^\circ, \frac{360^\circ}{D}, \dots, \frac{360(D-1)}{D}^\circ\}$ , where  $D$  is the number of uniform footstep directions. Then we compute the optimal-cost path from the initial to goal stance on this space using Anytime Repairing A\* (ARA\*) [46]. ARA\* requires a state transition cost function  $c(s_{j-1}, s_j)$ , and a heuristic cost-to-go function  $h(s_j)$ . It will find the optimal path to the goal given enough computation time and an admissible  $h$ . If interrupted anytime, then the algorithm still returns a sub-optimal path with provable bounds. Please refer to [46] for further details.

In our case the state transition cost  $c(s_{j-1}, s_j)$  is the minimum-energy transition between the two consecutive stances  $s_{j-1} = (f_{j-1}, f_j)$  and  $s_j = (f_j, f_{j+1})$ , given by:

$$\begin{aligned} c(s_{j-1}, s_j) &= \min_{p_j} E_{\text{COM}}(f_{j-1}, f_j, f_{j+1}, p_j) \\ &\text{subject to:} \\ &\text{RCOF}(f_{j-1}, f_j, f_{j+1}, p_j) < \min(\mu_{j-1}, \mu_j, \mu_{j+1}) \quad (4) \\ &\Psi(f_{j-1}, f_j, f_{j+1}, p_j) < 0 \\ &a < p_j < b \end{aligned}$$

Hence, even though states in A\* search are discretized stances, step parameters are computed from continuous optimization on the state transitions.

Regarding the heuristic  $h(s_j)$ , we set it equal to a lower bound on the cost from  $s_j$  to the goal which assumes no obstacles, optimal cost of transport and infinite friction. This way  $h(s_j)$  never overestimates the true cost to the goal (i.e. is admissible), as required for A\* optimality. We compute the bound as the minimum horizontal cost of transport times distance:

$$\begin{aligned} h(s_j) &= d_{xy}(s_j, s_{N-1}) \cdot \min_{f_k, f_{k+1}, p_k} \frac{E_{\text{COM}}(f_{k-1}, f_k, f_{k+1}, p_k)}{\|(x, y)_{k+1} - (x, y)_{k-1}\|} \\ &\text{subject to:} \quad (5) \\ &\Psi(f_{k-1}, f_k, f_{k+1}, p_k) < 0 \\ &a < p_k < b \end{aligned}$$

where  $d_{xy}(s_j, s_{N-1})$  is the Euclidean distance on the horizontal plane from stance  $s_j$  to stance  $s_{N-1}$  (i.e. the distance between left feet and the right feet summed). True costs to goal will actually be higher than (5) since optimal step parameters might not be feasible for the whole distance and more costly paths might be necessary due to kinematics constraints, obstacles, friction or slope.

In practice, we pre-compute and store on a hash table the results of equation (4) for a large number of footstep displacements and coefficients of friction. Similarly, we only need to solve the optimization

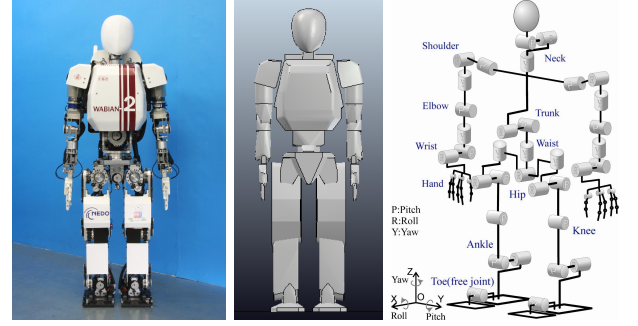


Fig. 1. The WABIAN-2 humanoid robot used in our simulation experiments. From left to right: real robot, simulated, DOF.

problem in (5) once. Planning a path from an initial stance  $s_1$  to a goal stance  $s_{N-1}$  then consists of a straightforward ARA\* (or A\*) search where each time a state transition is considered we:

- 1) access a hash table to obtain the state transition cost (4)
- 2) compute the heuristic cost-to-go from the distance to goal and the pre-computed cost-of-transport using (5).

### B. Implementation

We implement point cloud discretization with PCL [47] using 5cm grid-filtered point clouds. The search for successors of a stance is done by a range search of points around the fixed foot. Also, the directions of footsteps were discretized uniformly with  $D = 24$ .

We use the official implementation of ARA\* [46] in the Search-Based Planning Library (SBPL) [48]. The optimization problems (4) (5) are first solved with the global optimization algorithm DIRECT [49], which is then refined using the sequential quadratic programming algorithm SLSQP [50]. Both optimization algorithms are implemented in the NLOpt library [51]. The functions  $E_{\text{COM}}$ , RCOF and  $\Psi$  are each implemented as an infinite mixture of linear experts (IMLE) as described in Section IV-B.

During ARA\* search we use pre-computed versions of (4) for speed. After the final solution is obtained we further refine the step parameters  $p$  by solving (4) using SLSQP, warm-started by the values stored on the hash table.

## VI. RESULTS

### A. Platform and setup

All experiments described in this paper were conducted on a simulated model of humanoid robot WABIAN-2, shown in Figure 1. WABIAN-2 is a human-size humanoid robot, 1.5m tall, weighting 64kg and with 41 DOFs. Joints are driven by DC-motors with high gear reduction ratios of around 200. We used Open Dynamics Engine (ODE) for physics simulation on the V-REP robot simulator [53], at a 4ms control cycle (ODE computation time step 1ms, global ERP 0.8, all other parameters set to their default values). The robot's joints are position controlled using the same gains as the real robot (proportional gain between 0.7 and 0.8). We used the Walking Pattern Generator described in [44] which stabilizes the walking motion based on the robot's full dynamical model and works for varying COM height motion. ZMP reference trajectories were placed at the center of the stance foot during the swing phase and cubic-spline-interpolated to the other foot during the double support phase. Full trajectories of the knees were obtained by cubic spline interpolation between a minimum flexion angle at impact  $\phi_0$  and maximum flexion angle at stance  $\phi_{st}$  and swing  $\phi_{sw}$ , as shown in Fig. 2.

The limits of stance reachability were set according to the kinematic chain of WABIAN-2 by manual inspection:

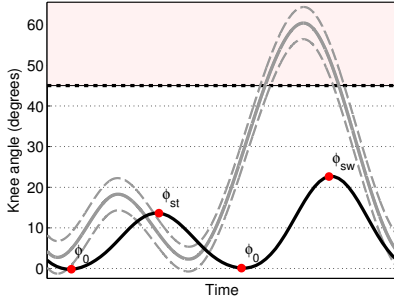


Fig. 2. Knee trajectories used for the robot are interpolated with a cubic spline between a minimum flexion angle  $\phi_0$  at impact and maximum angles at stance  $\phi_{st}$  and swing  $\phi_{sw}$ . Average and standard deviation of human data is plotted in gray based on [52]. The robot's curve can be made close to that of humans by adjusting double support time (moving  $\phi_0$  to the left in this example) and stance angle ( $\phi_{st}$  up), however  $\phi_{sw}$  cannot exactly match human data ( $\phi \leq 45^\circ$ , pink region is unfeasible).

- $\Delta x \in [0; 0.38]$  meters, where  $x$  points forward,
- $\Delta y \in [0.17; 0.30]$  meters, where  $y$  points to the left (symmetric interval if  $f_{j+1}$  is a right foot),
- $\Delta z \in [-0.15; 0.15]$  meters, where  $z$  points upward,
- $\Delta \theta \in [0; 30]$  degrees, where  $\theta$  runs counter-clockwise (symmetric interval if  $f_{j+1}$  is a right foot).

The state transition (i.e. step) parameter vector was defined as  $p = (\Delta t_{ds}, \Delta t_{sw}, \phi_0, \phi_{st}, \phi_{sw}) \in \mathbb{R}^5$ , and sampled within the intervals:

- $\Delta t_{ds} \in [0.09; 1.8]$ ;  $\Delta t_{sw} \in [0.9; 1.8]$  seconds,
- $\phi_0 \in [1; 21]$  degrees,
- $\phi_{st} \in [5; 45]$ ;  $\phi_{sw} \in [5; 45]$  degrees.

Due to the high dimensionality of the models, we had to obtain thousands of training points from simulations. To reduce training time we trained two separate versions of each model: one for level, one for inclined terrain. We used all dimensions except  $\Delta z$  on the level terrain version, and an approximate model on inclined terrain. In the latter, knee trajectories have a narrow feasibility space (collisions, complex motion) and so we constrained them such as to obtain a fixed foot-COM height trajectory. With this approximation, models were learned in around 2 days of simulation. In total we generated around 12,600 different walking patterns. Each pattern is a sequence of 6 symmetric steps of constant step length, width, height and  $p$ . From these simulations we gathered measurements of  $E_{COM}$ , RCOF and  $\Psi$ .

As explained in Section V, we then fitted an IMLE model to the measurements; solved (4) for a large number of footstep displacement and  $\mu$  values; and stored the results on a hash table. In our experiments this hash table had 18,491 entries. To solve (4) this many times took approximately 2 hours. When planning, we simply query the table to obtain state transition costs and step parameters  $p$  from the transitions' footstep displacement and  $\mu$  values. Query time is at the microsecond level.

### B. Models of energy and RCOF

Figure 3 shows the  $E_{COM}$  model as a function of step length and height, for two different slope friction values ( $\mu = 0.2$  and  $0.4$ ). The energy at each steplength-stepheight combination also depends on the other parameters  $p$ , and so the minimum  $E_{COM}$  across  $p$  is shown at each point. The gradient of the energy is mainly dominated by the step height value, indicating high energetic cost for slanted terrain. The maximum feasible slope angle for each friction value can be seen by the absence of colored energy values, and is approximately  $18^\circ$  for  $RCOF < 0.2$  and  $45^\circ$  for  $RCOF < 0.4$ . The high energetic cost

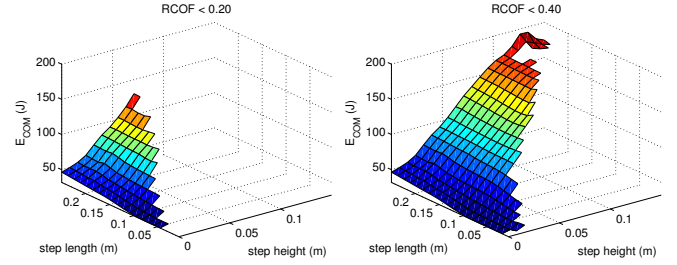


Fig. 3. Minimum  $E_{COM}$  on slopes, as a function of step length and step height. Measured in physics simulation.

of slanted terrain actually leads to a preference of shallow walking slopes as we will show in Section VI-C and VI-D. Figure 4 shows the contours of  $E_{COM}$  for level walking. The figure shows that most of the energy is spent in double support: the shorter  $\Delta t_{ds}$  the lower the energy. Leg swing time mostly does not influence COM energy, which reflects the fact that the alignment of velocity and force are low when compared to double support (motion on the sagittal plane is close to an inverted pendulum).

We show the RCOF model in Figure 5. RCOF is mainly dependent on the time spent in double support (contours are vertical in the right-most  $\Delta t_{ds}$ ,  $\Delta t_{sw}$  plot). The higher  $\Delta t_{ds}$  is, the lower the RCOF. Also, the lower the step length, the lower the RCOF. Our interpretation is that both increasing  $\Delta t_{ds}$  and decreasing step length lead to lower COM accelerations during double support and thus a more static gait, because of that tangential forces are lower and so is RCOF. These observations match human data as we will discuss in Section VI-D.

### C. $E_{COM}$ -optimal planning: resulting paths and energetic advantages

In this section we analyze the walking paths generated by the described  $E_{COM}$ -optimal planner in practice, as well as the paths' expected electrical energy consumption. Our motivation for estimating electrical energy consumption was not only due to its practical value in robotics, but also because mechanical work in humans is related to metabolic energy (i.e. oxygen consumption) [36], [29].

Since the real WABIAN-2's joints are driven by DC-motors [54], we compute electrical energy as

$$E_{ele} = \sum_i \left( \int_{t_0}^{t_1} |\tau_i \omega_i| dt + \int_{t_0}^{t_1} R_i I_i^2 dt \right) \quad (6)$$

where  $i$  is an index of the motor,  $\tau$  is motor torque and  $\omega$  angular velocity.  $I$  refers to current, which in simulation is computed as  $\tau / (r \cdot K_\tau)$ , where  $r$  is the motor's gear reduction ratio and  $K_\tau$  the torque constant, taken from the motors' data sheets.  $R I^2$  are the power losses due to motor armature resistance and we ignore mechanical losses such as joint friction.

We compare the resulting electrical energy consumption obtained by our planner with a set of baselines: 1) minimum-travel-time planner, 2) minimum-sum-of-torques planner, 3) directly optimizing electrical energy consumption  $E_{ele}$  as defined in (6). The results for the baselines were obtained using exactly the same planner equations (4) (5) and implementation, the only difference being that we replaced  $E_{COM}$  by  $(\Delta t_{ds} + \Delta t_{sw})$ ,  $\int \sum_i \tau_i^2 dt$ , and  $E_{ele}$  respectively.

We conducted the experiments in three different scenarios which we will now describe and analyze. Energy consumption results are reported in Table I.

The first scenario (Figure 6) was as follows: the robot stands in a ground with friction  $\mu_{ground} = 1.0$  and has to walk to a target which is straight ahead, 3m away. Between the start and finish points

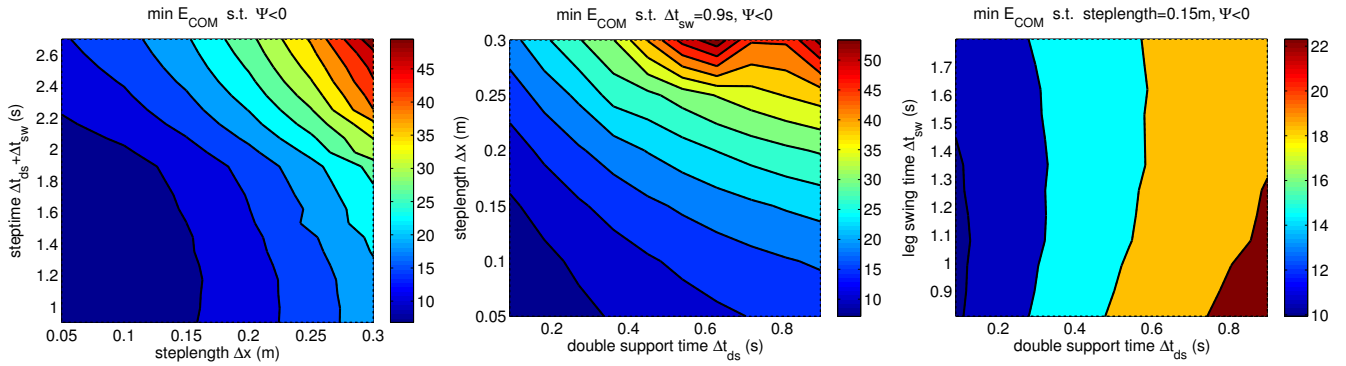


Fig. 4. Minimum  $E_{COM}$  measured in physics simulation, on flat terrain.

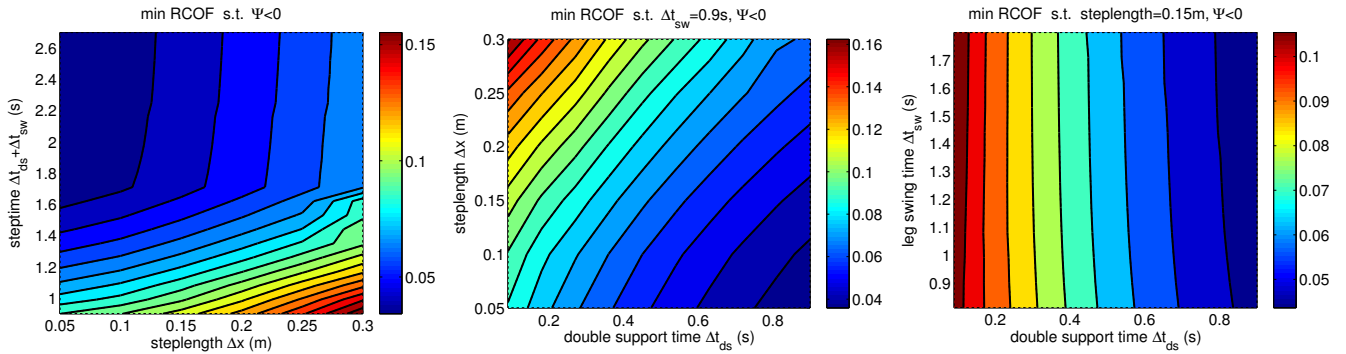


Fig. 5. RCOF, or the maximum ratio of tangential-to-normal force over a step, measured in physics simulation on flat terrain. It indicates the minimum ground coefficient of friction  $\mu$  where the robot can walk without slipping.

there is an "ice patch" of very low friction  $\mu_{ice}$ . We conducted several planning experiments with different  $\mu_{ice} \in \{0.12, 0.06\}$  and different widths of the ice patch ( $\{0.5, 1\}$ m). Figure 6 shows that using our planner the robot walked through the ice for  $\mu_{ice} = 0.12$  (specifically it walked 5% slower than the optimal speed with increased double support), but walked around the ice if  $\mu_{ice} = 0.06$ . When we doubled the ice patch width but kept the low friction  $\mu_{ice} = 0.06$ , the planner found it more optimal to go through the ice approximately twice as slow (with increased double support) than around a great distance. In terms of expected electrical energy (Table I), the paths generated by our planner spent 2110 J, 2427 J and 3031 J respectively. We also conducted experiments constraining the planner to take the alternative, sub-optimal choice of avoiding the ice patch when it is optimal to cross it and vice-versa. Such sub-optimal choices would lead to 14%, 19% and 10% more electrical energy respectively. Thus, an increase in COM work (sub-optimal plan) lead to an increase in electrical energy consumption. The electrical energy obtained by our optimal planner was relatively close to the real minimum of  $E_{ele}$ . Optimizing electrical energy directly lead to 25%, 12% and 18% less consumption than optimizing COM work. On the other hand, optimizing travel time (common objective function of footstep planners) would lead to drastic energy spending, increasing by 26%, 51% and 92%. Optimizing joint torques decreased energy spending slightly by 11%, 3% and 13%.

The second scenario (Figure 7) was as follows: there are two stairs at equal distance to the robot ( $x = 1$  meter away,  $y = \pm 0.50$ m), both ending at the same final height ( $z = 0.50$ m). One of the stairs has 3 high steps while the other has 6 lower steps. The goal of the robot is to reach a distant centered position  $(x, y, z) = (3, 0, 0.5)$ m. The energy cost should be the same if the stairs were identical. We show the obtained footstep plan in Figure 8. The figure shows that the

planner opts for the lower-but-many-step stairs. The reason for this result is that on steep stairs, steps become too costly for the distance traveled. Notice that the slope of the energetic cost  $E_{COM}$  in Figure 3 is high in the direction of step height. We will further analyze the cost of slanted locomotion in Section VI-D. In terms of expected electrical energy (Table I), our planner's path was 13% away from the true minimum of  $E_{ele}$ . The sub-optimal choice of taking the few-but-high stairs would increase consumption by 9%, and optimizing travel time would also increase consumption by 40%. Optimizing joint torques lead to basically the same performance as  $E_{COM}$  (0.5% more energy).

The final scenario was as follows: the robot has to climb a slope to a target which is straight ahead, 2.5m away measured on a straight line connecting the start and target points. The slope has an angle of  $\alpha \in \{10, 20, 25\}$  degrees. We show the planner results in Figure 8 and the simulation in Figure 7. The optimal path for the two shallowest slopes was in a straight line to the target, but for  $\alpha = 25^\circ$  the optimal path was curved and at a slightly lower inclination. These results match observations in human mountain paths as we will discuss in Section VI-D. In terms of expected electrical energy (Table I), our planner's path for the 25 degree slope is only 5% away from the true minimum of  $E_{ele}$ . The sub-optimal choice of taking a straight path to the target, instead of curved, would increase consumption by 1%. Optimizing travel time would increase consumption drastically by 97%. Obtaining a path by optimizing joint torques revealed to be unfeasible for our planner's time limit (which was 10 minutes), while an optimal plan was returned for  $E_{COM}$  in 10 seconds. By analyzing our model and planner data our conclusion is that the sum-of-torques function has high variance due to noise in simulated joint torque measurements, and its optimization is prone to get stuck in local optima. The electrical energy minimizing planner also includes

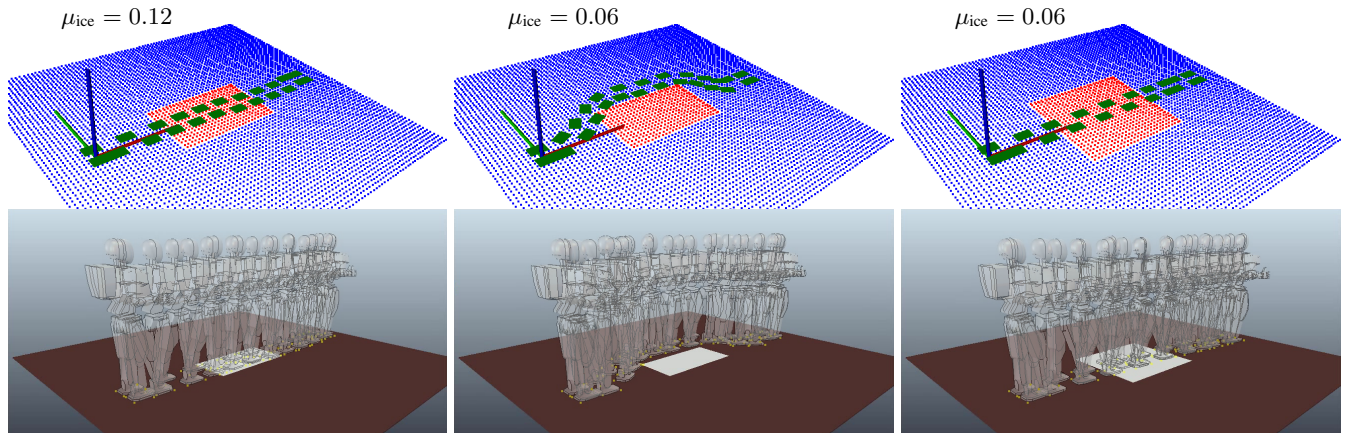


Fig. 6. Optimal plans obtained by our planner in the "ground and ice-patch" scenario. The top row shows the footstep plan and point cloud (red has friction  $\mu_{ice}$ , blue  $\mu_{ground} = 1$ ). Left: robot crosses a narrow ice patch ( $\mu_{ice} = 0.12$ ). Middle: robot walks around the patch if its slipperiness is increased ( $\mu_{ice} = 0.06$ ). Right: robot walks slowly through the same ice patch in case the ice is wider (energy spent avoiding it would be too high).

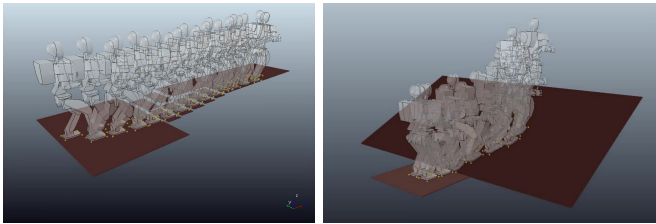


Fig. 7. Optimal plan obtained by our planner in the Stairs scenario (left), and Slope  $\alpha = 25^\circ$  scenario (right). Shallower stairs and slopes have lower cost.

a joint torques term and correspondingly also took longer to solve the path to optimality (177 seconds) than when using COM work.

For all scenarios our  $E_{COM}$ -optimal planner found a first sub-optimal path within 1 second and the optimal path within 1 minute. The computational speed improvement obtained by using pre-computed energy costs for different step-friction combinations was of around one order of magnitude for both the initial and optimal paths. The ODE-simulated robot successfully walked without falling in all situations, even at high slipperiness and slope levels.

From the optimal-vs-suboptimal experiments our results indicate that  $E_{COM}$  correlates well with  $E_{ele}$ . Still it was less susceptible to local minima and long planning times than  $E_{ele}$  or torque-minimization. These three quantities ( $E_{COM}$ ,  $E_{ele}$ , sum-of-torques) are all actually related with each other: Pearson correlation on data used for energy model training was  $r = 0.78$  between joint torques and  $E_{ele}$ ,  $r = 0.54$  between joint torques and  $E_{COM}$ ,  $r = 0.58$  between  $E_{COM}$  and  $E_{ele}$ , and  $r = 0.64$  between  $E_{COM}$  and joint mechanical work. Practically for our setup the human-inspired  $E_{COM}$  seems to be the best objective function choice as a compromise between energy consumption and computation time. Better optimization techniques could probably make direct optimization of  $E_{ele}$  more interesting, but in any case our proposed planner can be applied to both functions.

#### D. Comparison with human observations

The optimization objectives and variables proposed in this paper were inspired by human gait literature, as described in Section III. We now compare the results of our models and planner with the observations in human gait mentioned in that section.

**Gradient of mountain paths.** [29], [28] As we showed in model and planning results in Figure 3, 8 and 7, high  $E_{COM}$  of slanted

terrain leads to a preference of our planner towards shallower slopes. In our example scenarios, the robot took low-step stairs and a curved 20 degree path on a steep 25 degree slope. Likewise in humans, mountain paths are predicted by oxygen consumption experiments on slopes [29], [28]. According to [29], humans prefer to climb steep mountains at a maximum inclination of approximately 14 degrees, and in order to do that they climb not straight to the mountain peak but in a curved pattern. Mountain path observations are also partly reproduced by assuming minimization of COM mechanical work [29] which is our objective function in this paper. In Figure 9 we plot the chosen climbing angle versus the straight-line slope angle both for humans and our robot. The curve corresponding to humans was obtained by the data in [29]. The curve's shape is the same for humans and our robot: straight-line path until a certain angle, constant lower climbing angle after that. The angle at which this transition occurs is however different (approximately  $14^\circ$  for humans,  $20^\circ$  for the robot). We believe this to be due to differences in motor efficiency since WABIAN-2's weight, dimensions and joint positions are inspired by humans. We calculated the extra (constant) energy consumption of humans that would lead to the same plot as our robot's, and found it to be  $0.5\text{cal/kg/m}$ . This curve is also shown in Figure 9.

**Horizontal cost of transport.** [33], [35] The plots in Figure 4 showed energy consumption per step. A known result from human biomechanics is, however, on the energetic cost per distance (i.e. cost of transport). The contours of human oxygen consumption per meter in steplength-step-rate space actually resemble an hyperbola [33]. An empirical formula explaining this data was estimated by Zarrugh et al. [33], using which we computed the energy consumption of a human with WABIAN-2's physical limits (maximum step length 0.35m, maximum step rate 1.20). Figure 10 shows the humans' cost of transport prediction, as well as WABIAN-2's actual cost of transport (i.e. minimum  $E_{COM}$  per distance). The hyperbolic shape of the energy contours is similar to both humans and robot. The energy minimum seems to be slightly shifted towards a higher step rate in the robot's case, which we assume to be due to motor efficiency once again, although it could also be related to a lower range of motion of the knees in our robot (up to 45 instead of 60 degrees). The similar shape is not surprising since it has also been reproduced by computer simulations of a simple bipedal walking model [35] using COM work optimization during toe-off.

**Required Coefficient of Friction.** [20], [21], [27], [25] Figure 5, which shows the robot's RCOF model, also matches observations

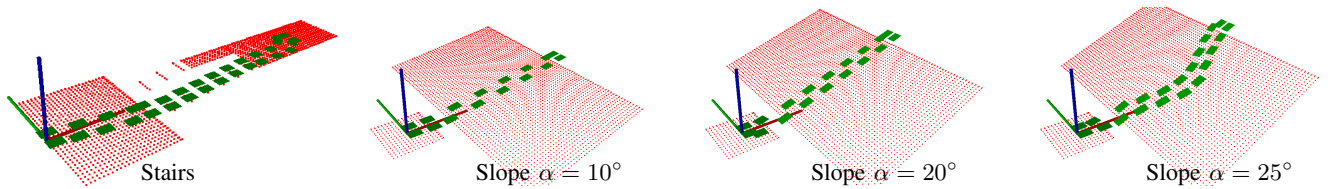


Fig. 8. Optimal plans obtained by our planner in the "Stairs" and "Slope" scenarios. On steep stairs and slopes, it is more energy optimal to walk a longer inclined distance but at a lower angle.

TABLE I  
ESTIMATED ELECTRICAL ENERGY CONSUMPTION OF OUR PLANNER USING DIFFERENT OBJECTIVE FUNCTIONS

Scenario	$E_{COM}$ (this paper)	Suboptimal $E_{COM}$	Travel time	Sum-of-torques	$E_{ele}$ (ideal energy consumption)
Narrow ice $\mu = 0.12$	2110 J	+14%	+26%	-11%	-25%
Narrow ice $\mu = 0.06$	2427 J	+19%	+51%	-3%	-12%
Wide ice $\mu = 0.06$	3031 J	+10%	+92%	-13%	-18%
Stairs $\mu = 1$	4116 J	+9%	+40%	+0.5%	-13%
Slope $\mu = 1, \alpha = 25^\circ$	4908 J	+1%	+97%	(failed)	-5%

\*Note: Reported energy is the estimated electrical energy consumption (6). Percentage values represent additional energy as a percentage of  $E_{COM}$  (i.e.  $(E' - E_{COM})/E_{COM}$ ). "Suboptimal  $E_{COM}$ ": refers to a plan that takes a sub-optimal navigation option (i.e. around the ice instead of through; through instead of around; using the few-but-high-step stairs; walking straight on a  $25^\circ$  slope instead of in a curve) although still optimizing  $E_{COM}$  given that constraint.

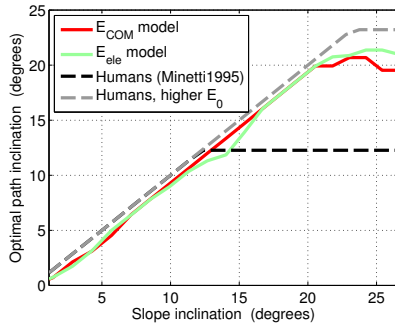


Fig. 9. Optimal path inclination angle  $\alpha_{path}$  as a function of the slope angle  $\alpha$ . If  $\alpha_{path} < \alpha$  then the path is curved at shallower inclination and longer total distance.

in human gait. The figure shows that the higher  $\Delta t_{ds}$  is, the lower the RCOF. And also the lower the step length, the lower the RCOF. According to [21] humans reduce RCOF (the shear-to-normal force ratio) when walking on slippery terrain, which in our planner we assume to be a walking constraint such that  $RCOF < \mu$ . The higher double support observation means that to be able to walk on more slippery terrain (lower RCOF) the robot should opt for a conservative gait that is more static, with lower tangential speeds and accelerations. Also in humans a "cautious", more static, gait has been observed in humans walking on slippery terrain [20], [21], [22], as referred in Section II-B. On the other hand [27] specifically observed an increase in double support time when walking on slippery terrain. Regarding step length, [20], [21], [25] also observed that this variable is lower when humans walk on slippery terrain. Reduction of step length is actually an anticipation strategy used just before stepping on slippery terrain [20], [21], [25], just as in our robot's case it is planned by assuming a constraint on RCOF [21]. While our planner uses a hard RCOF constraint, the decision was mainly motivated for practical and conservative reasons: a hard constraint lowers the risk of falling by theoretically avoiding slippage completely and thus not having to rely heavily on reactive slippage control. Humans, on the other hand, could possibly use RCOF or a related metric as a soft constraint, although we are not aware of any investigation on these lines.

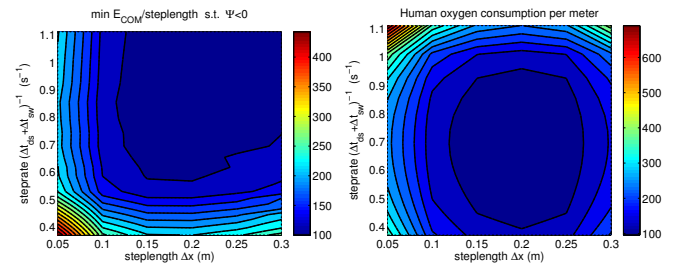


Fig. 10. Left: Our robot's minimum  $E_{COM}$  per distance traveled. Right: Oxygen consumption of a human with WABIAN-2's physical limits, given by the empirical formulas of human walking of [33]. Units are in percentage of the minimum.

## VII. CONCLUSIONS AND DISCUSSION

In this paper we showed that optimal footstep planning for humanoid robots, by using simple principles and gait representations from human gait literature, leads to both human-like walking behavior and low electrical power consumption. Importantly, we showed through several simulation experiments that the planner we proposed here is well suited for challenging outdoor scenarios since it accounts for ground friction and energy consumption.

We proposed a footstep planning algorithm with a human-inspired objective (COM work), constraint (RCOF) and variables (step length, width, height, double support time, swing time and knee flexion). We showed that our models and planner lead to a number of interesting observations such as: human-like RCOF, step length and double support time changes on slippery terrain, human-like curved walking on steep slopes after  $20^\circ$ , and hyperbolic contours of energy per distance in steplength-steprate plots. By estimating DC-motor electrical power consumption from simulation data, we also showed that planned paths had close to optimal electrical consumption, and that higher COM work leads to higher electrical energy. These observations and the simplicity of the model suggest COM work to be an effective objective function for planning of robot locomotion.

Some points in this paper may be important to discuss:

**Footstep planning with a learned model.** Our footstep planner relies on learned models of energy and slippage to plan optimal footstep sequences. These models depend on both the robot and whole-body controller used. Therefore, the models we obtained might

differ from the ones obtained with different robots or using different controllers. The approach is still general, and all that is required to apply our planner is to learn the  $E_{\text{COM}}$ , RCOF,  $\Psi$  models in simulation with the desired robot and controller.

**Energy consumption.** We show that COM work is related to electrical energy consumption. However, at the cost of using a more complex model, further energy savings can be obtained by directly optimizing energy consumption. Also, an interesting extension of our work would be to use the footstep planner's path as an initialization to a full-body trajectory optimization algorithm with the same objective.

**Coefficient of friction estimation.** The planner proposed here relies on the knowledge of the coefficient of friction between robot foot and the ground. While its estimation might be difficult in practice, we believe material classification from images and tabled COFs to be a feasible approach to the problem. Also, the planner can still be applied when uncertainty in the estimation is considered. For example, a margin can be added to the RCOF constraint depending on the expected uncertainty.

**Feasibility model.** The use of a feasibility model learned in simulation was crucial in our experiments. One of the problems in footstep planning is to generate a plan for which whole-body motion is feasible. In practice we found heuristic limits on stance distances to be insufficient due to unmodeled kinematics and dynamic unfeasibility. Learning feasibility as a function of step parameters alleviated this problem and sped up planning considerably since more stances and steps were discarded early on.

**Planning footstep timing.** This paper importantly shows that planning time variables along with footstep placement is crucial when including ground friction in the problem. The required coefficient of friction (RCOF) for a slip to occur decreases with the decrease of step length and with the increase of double support time, thus allowing the robot to walk on very slippery surfaces by adjusting these variables (as happens with humans [20], [21], [25], [27]). This also contrasts to the common practice in humanoid robotics to use constant step times.

**Search speed.** We compute parameters other than footstep placement from state transitions, which reduces the A\* search space and increases search speed. Pre-computing energetic cost for many combinations of footstep placement and  $\mu$  also allowed for faster search than if (4) were to be solved explicitly for each state expansion. Instead we solve it only for the final obtained path, reducing computation speed by one order of magnitude. Also, in this paper collision checking was not necessary due to the absence of obstacles in the tested scenarios. We expect current computational times to increase when adding a collision checking algorithm to the problem.

#### ACKNOWLEDGMENT

This work was supported by JSPS KAKENHI (Grant Number 15J06497 and 25220005) and ImPACT TRC Program of Council for Science, Technology and Innovation (Cabinet Office, Government of Japan). It was also supported by the projects FCT [UID/EEA/50009/2013] and EU Poeticon++.

#### REFERENCES

- [1] M. Brandao, K. Hashimoto, J. Santos-Victor, and A. Takanishi, "Gait planning for biped locomotion on slippery terrain," in *14th IEEE-RAS International Conference on Humanoid Robots*, November 2014, pp. 303–308.
- [2] —, "Optimizing energy consumption and preventing slips at the footstep planning level," in *15th IEEE-RAS International Conference on Humanoid Robots*, Nov 2015, pp. 1–7.
- [3] W. Huang, J. Kim, and C. Atkeson, "Energy-based optimal step planning for humanoids," in *2013 IEEE International Conference on Robotics and Automation*, May 2013, pp. 3124–3129.
- [4] J. Kim, N. Pollard, and C. Atkeson, "Quadratic encoding of optimized humanoid walking," in *13th IEEE-RAS International Conference on Humanoid Robots*, Oct 2013, pp. 300–306.
- [5] J. Chestnutt, M. Lau, G. Cheung, J. Kuffner, J. Hodgins, and T. Kanade, "Footstep planning for the honda asimo humanoid," in *2005 IEEE International Conference on Robotics and Automation*, April 2005, pp. 629–634.
- [6] J. Garimort and A. Hornung, "Humanoid navigation with dynamic footstep plans," in *2011 IEEE International Conference on Robotics and Automation*, May 2011, pp. 3982–3987.
- [7] A. Hornung, A. Dornbush, M. Likhachev, and M. Bennewitz, "Anytime search-based footstep planning with suboptimality bounds," in *12th IEEE-RAS International Conference on Humanoid Robots*, Nov 2012, pp. 674–679.
- [8] K. Hauser, T. Bretl, J.-C. Latombe, K. Harada, and B. Wilcox, "Motion planning for legged robots on varied terrain," *The International Journal of Robotics Research*, vol. 27, no. 11-12, pp. 1325–1349, 2008.
- [9] H. Dai, A. Valenzuela, and R. Tedrake, "Whole-body motion planning with centroidal dynamics and full kinematics," in *14th IEEE-RAS International Conference on Humanoid Robots*, Nov 2014, pp. 295–302.
- [10] R. Deits and R. Tedrake, "Footstep planning on uneven terrain with mixed-integer convex optimization," in *14th IEEE-RAS International Conference on Humanoid Robots*, Nov 2014, pp. 279–286.
- [11] K. Hauser, T. Bretl, K. Harada, and J.-C. Latombe, "Using motion primitives in probabilistic sample-based planning for humanoid robots," in *Algorithmic foundation of robotics VII*. Springer, 2008, pp. 507–522.
- [12] N. Perrin, O. Stasse, L. Baudouin, F. Lamiraux, and E. Yoshida, "Fast humanoid robot collision-free footstep planning using swept volume approximations," *IEEE Transactions on Robotics*, vol. 28, no. 2, pp. 427–439, April 2012.
- [13] S. Kajita, K. Kaneko, K. Harada, F. Kanehiro, K. Fujiwara, and H. Hirukawa, "Biped walking on a low friction floor," in *2004 IEEE/RSJ International Conference on Intelligent Robots and Systems*, vol. 4, Sept 2004, pp. 3546–3552 vol.4.
- [14] J. H. Park and O. Kwon, "Reflex control of biped robot locomotion on a slippery surface," in *2001 IEEE International Conference on Robotics and Automation*, vol. 4, 2001, pp. 4134–4139 vol.4.
- [15] M. Nikolic, B. Branislav, and M. Rakovic, "Walking on slippery surfaces: Generalized task-prioritization framework approach," in *Advances on Theory and Practice of Robots and Manipulators*, ser. Mechanisms and Machine Science, M. Ceccarelli and V. A. Glazunov, Eds. Springer International Publishing, 2014, vol. 22, pp. 189–196.
- [16] S. Feng, X. Xinjilefu, W. Huang, and C. Atkeson, "3d walking based on online optimization," in *13th IEEE-RAS International Conference on Humanoid Robots*, October 2013.
- [17] S. Kajita, F. Kanehiro, K. Kaneko, K. Fujiwara, K. Harada, K. Yokoi, and H. Hirukawa, "Biped walking pattern generation by using preview control of zero-moment point," in *2003 IEEE International Conference on Robotics and Automation*, vol. 2, Sept 2003, pp. 1620–1626 vol.2.
- [18] E. J. Gibson, G. Riccio, M. A. Schmuckler, T. A. Stoffregen, D. Rosenberg, and J. Taormina, "Detection of the traversability of surfaces by crawling and walking infants." *Journal of Experimental Psychology: Human Perception and Performance*, vol. 13, no. 4, p. 533, 1987.
- [19] K. E. Adolph, A. S. Joh, and M. A. Eppler, "Infants' perception of affordances of slopes under high-and low-friction conditions." *Journal of Experimental Psychology: Human Perception and Performance*, vol. 36, no. 4, p. 797, 2010.
- [20] G. Cappellini, Y. P. Ivanenko, N. Dominici, R. E. Poppele, and F. Lacquaniti, "Motor patterns during walking on a slippery walkway," *Journal of Neurophysiology*, vol. 103, no. 2, pp. 746–760, 2010.
- [21] R. Cham and M. S. Redfern, "Changes in gait when anticipating slippery floors," *Gait & Posture*, vol. 15, no. 2, pp. 159 – 171, 2002.
- [22] T. L. Heiden, D. J. Sanderson, J. T. Inglis, and G. P. Siegmund, "Adaptations to normal human gait on potentially slippery surfaces: The effects of awareness and prior slip experience," *Gait & Posture*, vol. 24, no. 2, pp. 237 – 246, 2006.
- [23] J. G. Buckley, K. J. Heasley, P. Twigg, and D. B. Elliott, "The effects of blurred vision on the mechanics of landing during stepping down by the elderly," *Gait & Posture*, vol. 21, no. 1, pp. 65 – 71, 2005.
- [24] H. B. Menz, S. R. Lord, R. S. George, and R. C. Fitzpatrick, "Walking stability and sensorimotor function in older people with diabetic peripheral neuropathy1," *Archives of Physical Medicine and Rehabilitation*, vol. 85, no. 2, pp. 245 – 252, 2004.
- [25] J. C. Menant, J. R. Steele, H. B. Menz, B. J. Munro, and S. R. Lord, "Effects of walking surfaces and footwear on temporo-spatial gait parameters in young and older people," *Gait & Posture*, vol. 29, no. 3, pp. 392 – 397, 2009.

- [26] A. J. Chambers, S. Margerum, M. S. Redfern, and R. Cham, "Kinematics of the foot during slips," *Occupational Ergonomics*, vol. 3, no. 4, pp. 225–234, 2002.
- [27] M. G. A. Llewellyn and V. R. Nevola, "Strategies for walking on low-friction surfaces," in *The Fifth International Conference on Environmental Ergonomics*. Maastricht, 1992, pp. 156–157.
- [28] R. M. Alexander, *Principles of animal locomotion*. Princeton University Press, 2003.
- [29] A. Minetti, "Optimum gradient of mountain paths," *Journal of Applied Physiology*, vol. 79, no. 5, pp. 1698–1703, 1995.
- [30] D. R. Proffitt, M. Bhalla, R. Gossweiler, and J. Midgett, "Perceiving geographical slant," *Psychonomic Bulletin & Review*, vol. 2, no. 4, pp. 409–428, 1995.
- [31] J. M. Wang, D. J. Fleet, and A. Hertzmann, "Optimizing walking controllers for uncertain inputs and environments," *ACM Trans. Graph.*, vol. 29, no. 4, pp. 73:1–73:8, Jul. 2010.
- [32] D. A. Winter, *Biomechanics and motor control of human gait: normal, elderly and pathological*, 2nd ed., 1991.
- [33] M. Zarrugh, F. Todd, and H. Ralston, "Optimization of energy expenditure during level walking," *European Journal of Applied Physiology and Occupational Physiology*, vol. 33, no. 4, pp. 293–306, 1974.
- [34] A. Minetti and R. Alexander, "A theory of metabolic costs for bipedal gaits," *Journal of Theoretical Biology*, vol. 186, no. 4, pp. 467–476, 1997.
- [35] A. D. Kuo, "A simple model of bipedal walking predicts the preferred speed–step length relationship," *Journal of biomechanical engineering*, vol. 123, no. 3, pp. 264–269, 2001.
- [36] B. R. Umberger and P. E. Martin, "Mechanical power and efficiency of level walking with different stride rates," *Journal of Experimental Biology*, vol. 210, no. 18, pp. 3255–3265, 2007.
- [37] K. Sasaki, R. R. Neptune, and S. A. Kautz, "The relationships between muscle, external, internal and joint mechanical work during normal walking," *Journal of Experimental Biology*, vol. 212, no. 5, pp. 738–744, 2009.
- [38] D. A. Winter, "A new definition of mechanical work done in human movement," *Journal of Applied Physiology*, vol. 46, no. 1, pp. 79–83, 1979.
- [39] J. S. Matthis and B. R. Fajen, "Humans exploit the biomechanics of bipedal gait during visually guided walking over complex terrain," *Proceedings of the Royal Society of London B: Biological Sciences*, vol. 280, no. 1762, p. 2013, 2013.
- [40] H. B. Menz, S. R. Lord, and R. C. Fitzpatrick, "Acceleration patterns of the head and pelvis when walking on level and irregular surfaces," *Gait & Posture*, vol. 18, no. 1, pp. 35–46, 2003.
- [41] D. Fong, Y. Hong, and J. X. Li, "Lower-extremity gait kinematics on slippery surfaces in construction worksites," *Medicine and science in sports and exercise*, vol. 37, no. 3, pp. 447–454, 2005.
- [42] K. Mombaur, A. Truong, and J.-P. Laumond, "From human to humanoid locomotion an inverse optimal control approach," *Autonomous robots*, vol. 28, no. 3, pp. 369–383, 2010.
- [43] S. Collins and A. Ruina, "A bipedal walking robot with efficient and human-like gait," in *2005 IEEE International Conference on Robotics and Automation*, April 2005, pp. 1983–1988.
- [44] K. Hashimoto, H. Kondo, H.-O. Lim, and A. Takahashi, *Motion and Operation Planning of Robotic Systems: Background and Practical Approaches*. Springer International Publishing, 2015, ch. Online Walking Pattern Generation Using FFT for Humanoid Robots, pp. 417–438.
- [45] B. Damas and J. Santos-Victor, "Online learning of single-and multi-valued functions with an infinite mixture of linear experts," *Neural computation*, vol. 25, no. 11, pp. 3044–3091, 2013.
- [46] M. Likhachev, G. J. Gordon, and S. Thrun, "Ara\*: Anytime a\* with provable bounds on sub-optimality," in *Advances in Neural Information Processing Systems*, 2003, p. None.
- [47] R. B. Rusu and S. Cousins, "3D is here: Point Cloud Library (PCL)," in *2011 IEEE International Conference on Robotics and Automation*, Shanghai, China, May 9-13 2011.
- [48] M. Likhachev. (2010) Search-based planning library. [Online]. Available: <http://www.ros.org/wiki/sbpl>
- [49] D. R. Jones, C. D. Perttunen, and B. E. Stuckman, "Lipschitzian optimization without the lipschitz constant," *Journal of Optimization Theory and Applications*, vol. 79, no. 1, pp. 157–181, 1993. [Online]. Available: <http://dx.doi.org/10.1007/BF00941892>
- [50] D. Kraft, "Algorithm 733: Tomp–fortran modules for optimal control calculations," *ACM Transactions on Mathematical Software*, vol. 20, no. 3, pp. 262–281, Sep 1994.
- [51] S. G. Johnson. The nlopt nonlinear-optimization package. [Online]. Available: <http://ab-initio.mit.edu/nlopt>
- [52] J. Perry, *Gait analysis: normal and pathological function*. Slack Incorporated, 1992.
- [53] M. Freese, S. Singh, F. Ozaki, and N. Matsuhira, "Virtual robot experimentation platform v-rep: A versatile 3d robot simulator," in *Simulation, Modeling, and Programming for Autonomous Robots*, ser. Lecture Notes in Computer Science. Springer, 2010, vol. 6472, pp. 51–62.
- [54] E.-C. Corporation, *DC Motors, Speed Controls, Servo Systems*. Pergamon, 1977.



**Martim Brandão** received his M.Sc. in Electrical and Computer Engineering from Instituto Superior Técnico (IST, Portugal) in 2010. He was a Research Assistant at the Computer and Robot Vision Lab (IST) in 2011, and a Research Student at Takahashi Laboratory (Waseda University, Japan) until 2013. He is now a Ph.D. student at Waseda University. His research focuses on human-inspired robot motion planning, as well as vision-related topics for robot locomotion.



**Kenji Hashimoto** is an Assistant Professor of the Waseda Institute for Advanced Study, Waseda University, Japan. He received the B.E. and M.E. in Mechanical Engineering in 2004 and 2006, respectively, and the Ph.D. in Integrative Bioscience and Biomedical Engineering in 2009, all from Waseda University, Japan. His research interests include walking systems, biped robots, and humanoid robots.



**José Santos-Victor** received a Ph.D. in Electrical and Computer Engineering in 1995 from Instituto Superior Técnico (IST, Portugal), in Computer Vision and Robotics. He is a Full Professor at IST and a researcher of the Institute for Systems and Robotics, Lisbon, where he founded the Computer and Robot Vision Lab. He is interested in Computer and Robot Vision, particularly visual perception and the control of action, and biologically inspired vision and robotics.



**Atsuo Takahashi** is a Professor of the Department of Modern Mechanical Engineering, Waseda University and director of the Humanoid Robotics Institute (HRI), Waseda University, Japan. He received the B.S.E. in 1980, M.S.E. in 1982 and Ph.D. in 1988, all in Mechanical Engineering from Waseda University. His current research is related to Humanoid Robots and its applications in medicine and well-being.